

Temperature dependence of the enthalpy and the heat capacity of the liquid-crystal octylcyanobiphenyl (8CB)

J. Thoen, H. Marynissen, and W. Van Dael

Laboratorium voor Molekulfysika, Katholieke Universiteit Leuven, B-3030 Leuven, Belgium

(Received 14 June 1982)

An adiabatic scanning calorimeter has been used to study the thermal behavior of the liquid-crystal octylcyanobiphenyl (8CB) in the temperature range between 10 and 50°C. The solid-to-smectic-*A* (*KA*), the smectic-*A*-to-nematic (*AN*), as well as the nematic-to-isotropic (*NI*) phase transitions, which fall in this temperature range, have been investigated in great detail. From our measuring procedure the enthalpy behavior (including latent heats) as well as the heat capacity have been obtained. For the *KA* transition the latent heat was 25.7 ± 1.0 kJ/mol and for the *NI* transition it was 612 ± 5 J/mol. Within the resolution of our experiment we find that the *AN* transition is a continuous one. For the latent heat, if any, we arrive at an upper limit of 0.4 J/mol (or 1.4×10^{-3} J/g). The observed anomaly in the heat capacity for the *AN* transition is not consistent with a nearly logarithmic singularity as predicted by the *XY* model, instead we obtain a critical exponent $\alpha = \alpha' = 0.31 \pm 0.03$. This result is consistent with the anisotropic scaling relation $\nu_{\parallel} + 2\nu_{\perp} = 2 - \alpha$. The pretransitional effects near the *NI* transition are in qualitative agreement with the hypothesis of quasitricritical behavior.

I. INTRODUCTION

Liquid crystals are composed of large asymmetric molecules which do not melt in a single stage from the anisotropic solid state to an isotropic liquid. A variety of mesophases with symmetries and properties intermediate between those of a crystal and a liquid can be present. Differences in orientational and spatial ordering of the molecules define the mesophases. Two of the more common intermediate phases between the crystal (*K*) and the isotropic (*I*) liquid are the nematic (*N*) and the smectic-*A* (*A*) phases. The nematic phase has the translational symmetry of a fluid but a broken rotational symmetry characterized by long-range orientational order produced by the alignment of the molecular axes along a unit vector called the director. In the nematic phase the centers of mass of the molecules are thus randomly positioned. This is not the case in the smectic-*A* phase which has a layered structure with layer planes perpendicular to the director. Within the layers there is no long-range order in the position of the centers of mass of the molecules. The layered structure of the smectic phase can be described by a one-dimensional mass density wave^{1,2} with a wave number *q* related to the layer spacing, and a complex amplitude ψ , which can be considered as a smectic-order parameter.

During recent years there has been considerable

interest in the study of phase transitions in liquid crystals. In particular, the smectic-*A*-nematic (*AN*) transition has recently been vigorously investigated in an effort to determine the order of the transition and the universality class for the critical behavior. The mean-field theories of McMillan² and Kobayashi¹ have, indeed, predicted that the *AN* transition can be either first order or second order with a tricritical point, where the transition changes from first to second order, occurring at a certain value of the ratio of the nematic-smectic-*A* transition temperature to the nematic-isotropic transition temperature T_{AN}/T_{NI} . In a given homologous series, e.g., this ratio depends on the number of carbon atoms in the alkyl chain. Further theoretical progress was made by de Gennes,³ who introduced a Landau-Ginsburg functional closely related to that of a superconductor. Based on this analogy it was suggested that the *AN* transition should belong to the same universality class as a superfluid, and should exhibit three-dimensional *XY* critical behavior, with the following critical exponent values⁴: $\alpha \simeq -0.02$, $\gamma \simeq 1.32$, and $\nu \simeq 0.67$. From the beginning, however, it was recognized that the analogy with the superconductor is only partial. Important differences are, e.g., the fact that the smectic phase does not have a true long-range order,⁵ and also that the free energy density associated with director splay deformations is not gauge in-

variant.⁶ More recently, renormalization-group techniques have been applied to the normal to superconducting transition and, along the same line of thinking as indicated by de Gennes, the results may be extended to the AN transition in liquid crystals. Halperin *et al.*⁷ showed that, to the first-order expansion in ϵ near four dimensions, the coupling between the director fluctuations and the smectic-order parameter makes the transition always weakly first order. In later work, however, Dasgupta and Halperin⁸ questioned the validity of this result for the three-dimensional case. They found that a lattice model for a superconductor had a phase transition asymptotically equivalent to that of a superfluid with an inverted temperature axis and showed no first-order effect. From a model by Helfrich,⁹ describing the AN transition as a melting process of a one-dimensional structure by thermally generated free dislocation loops, also no evidence for a first-order nature of the AN transition was found. Another interesting aspect of this model is that it allows anisotropic critical behavior with different critical exponents ν for the correlation length in a direction parallel (ξ_{\parallel} with ν_{\parallel}) or perpendicular (ξ_{\perp} with ν_{\perp}) to the director. In subsequent work by Nelson and Toner¹⁰ it was argued that dislocation mediated AN "melting" implies

$$\nu_{\parallel} = 2\nu_{\perp} . \quad (1.1)$$

Anisotropic critical behavior was also predicted by Lubensky *et al.*^{11–14} applying renormalization-group methods on a gauge-transformed de Gennes Hamiltonian³ for the AN transition: they found a series of crossovers from mean-field behavior to an anisotropic critical regime, further to an isotropic critical regime, and ultimately to a very weak first-order transition. In the anisotropic regime the following scaling relation holds¹¹:

$$2 - \alpha = \nu_{\parallel} + 2\nu_{\perp} , \quad (1.2)$$

with α the critical exponent describing the specific-heat anomaly. Nelson and Toner¹⁰ discuss the conflict between their result (1.1) and the asymptotic isotropic behavior predicted by Lubensky and Chen.¹¹ They argue that there is, in the renormalization-group results of Lubensky and Chen, another fixed point, which although physically inaccessible near $d=4$ to lowest order in ϵ , has precisely the anisotropy obtained for the dislocation-loop model. Consequently, both approaches could possibly be reconciled, provided that this fixed point becomes physically accessible and stable for $d=3$.

Recently a series of high-resolution calorimetric,^{15–25} x-ray scattering^{26,27} and light scattering^{26,28} measurements, to probe the critical behavior near the AN transition, have been carried out. Although bilayer smectics like cyanobenzylidene-octyloxyaniline (CBOOA), octyloxycyanobiphenyl (8OCB), and octylcyanobiphenyl (8CB) have been most extensively studied, recently some single-layer materials like some members of the $\bar{n}S5$ and $nO.m$ homologous series have also been investigated. In particular, 4-*n*-pentyl-phenylthiol-4'-octylbenzoate ($\bar{8}S5$) and butyloxybenzylidene-octylaniline (4O.8) have been studied in detail with several techniques. There does not seem to be a substantial difference between the bilayer and the single-layer smectics. In a recent comparison of the x-ray scattering and calorimetric results for 8OCB and 4O.8 by Birgeneau *et al.*²⁷ it was concluded that for both materials the following set of critical exponents was consistent with the data: $\gamma \simeq 4/3$, $\nu_{\parallel} \simeq 2/3$, $\nu_{\perp} \simeq 0.5$, and $\alpha = \alpha' \simeq 0.2$. These exponents are consistent with the anisotropic hyperscaling relation¹¹ (1.2). Some of the exponents (γ and ν_{\parallel}) are consistent with the values of the XY model but α and ν_{\perp} are definitely not. It is, however, also clear that the experimental correlation length exponents ν_{\parallel} and ν_{\perp} do not satisfy the anisotropic scaling relation (1.1) obtained by Nelson and Toner.¹⁰ It was also found that the amplitudes of the heat capacity and the correlation lengths in both materials satisfy two-scale-factor universality.²⁹

The nematic-isotropic (NI) transition is usually described in terms of the Landau–de Gennes³⁰ mean-field theory. On the basis of this theory it is expected that the NI transition should be weakly first order, as observed experimentally. For the behavior of the pretransitional effects, classical mean-field exponents are of course predicted. Since the molecular interactions are short range in liquid crystals, it would be more likely that nonclassical critical exponents, as for normal second-order critical points, would apply. Experimentally many physical quantities seem, however, to be rather well described by mean-field exponents.³¹ It has been suggested by Keyes³² that tricritical exponents should be expected for this transition, rather than the exponents predicted by the Landau–de Gennes mean-field theory. According to the conjectures of Keyes, two competing nematic-order parameters (the uniaxial one and a biaxial one) are expected to exhibit diverging fluctuations near T_{NI} even though the biaxial order parameter is zero in the nematic

phase. It is expected that the tricritical point can be reached in the presence of a suitable external field (e.g., a magnetic or an electric field for negative anisotropic magnetic or electric susceptibilities).^{32,33} Very recently Van Hecke and Stecki³⁴ suggested that tricritical behavior could also be associated with a mechanical instability present in a mean-field description of the pressure-density isotherms of a nematic liquid crystal. Experimental data do not in many cases allow an answer to this question because several exponent values are identical for the mean-field critical and the tricritical system. However, the gap exponent in *p*-methoxy-benzylidene-*p*-butylaniline (MBBA)³⁵ and the order-parameter exponent^{32,36} in several systems seem to be consistent only with the tricritical values. Also, the pretransitional enhancement observed in the isotropic phase for the heat capacity C_p seems to point towards the tricritical hypothesis.³⁷⁻⁴⁰

In this paper we describe a calorimetric investigation of the liquid-crystal octyloxybiphenyl (8CB) by means of an adiabatic scanning calorimeter, which we have previously used for measurements in fluids belonging to the universality class of the three-dimensional Ising model.⁴¹⁻⁴³ Data have been taken in the nematic- and smectic-*A* mesophases, as well as in the solid and in the isotropic liquid phases. Special attention has been given to the three (*KA*, *AN*, and *NI*) phase transitions. As will be pointed out in the next section, our measurement procedure allows us to obtain detailed information on the temperature dependence of the enthalpy (including latent heats) and of the heat capacity. This is of course an important advantage compared to the ac-calorimetric method, where no latent heats can be measured,⁴⁴ and differential scanning calorimetry (DSC), where true latent heats can hardly be distinguished from pretransitional increases of the heat capacity.¹⁹ This will be discussed in more detail in Sec. III.

This paper is organized in the following way. Section II describes the experimental method and apparatus. The experimental results are presented in Sec. III. A discussion of the latent-heat results is included there. Section IV gives a detailed account and discussion of the least-squares fitting results for the pretransitional effects near the *AN* and *NI* transitions. A summary and conclusions are given in Sec. V.

II. EXPERIMENTAL METHOD AND APPARATUS

The experimental results described in this paper were obtained by means of an adiabatic scanning

calorimeter. We have previously used an essentially identical apparatus for a detailed investigation of the critical behavior of the specific heat near the consolute point of binary and ternary mixtures.⁴¹⁻⁴³ Full details of the construction and on the different modes of operation are given elsewhere.⁴⁵ Here we will limit ourselves to a short account of the heating rate method and to a description of the sample cell used in this experiment with 8CB.

The calorimeter consists of four stages: a central one (the sample cell with the sample) and three outer shielding stages. All stages are of good heat-conducting materials and thermally insulated from each other. If a measured heating power P is applied continuously to stage 1, it can be easily verified that the total heat capacity C_1 of stage 1, being the sum of that of the sample (C_s) plus that of the holder (C_h), is given by

$$C_1 = C_h + C_s = P/\dot{T}, \quad (2.1)$$

provided that there is no net heat flow between stage 1 and the surrounding stage 2. In order to satisfy this condition to a high degree of accuracy, the temperature of stage 2 is forced to follow at all times the temperature of stage 1 by means of a servosystem with very high sensitivity. For stability reasons the temperature of two additional outer stages is also controlled with servosystems (for more details see Ref. 45).

In Fig. 1 the design of the sample holder is shown. It is made of copper, and gold plated inside and outside. The electric heater, which is mounted inside the cell, is a 1-m long thin-walled stainless-steel tube of 1-mm diameter containing a heating wire embedded in magnesium oxide insulating material. A stirring system is also built into the sample cell. The stirring is achieved by including in the sample holder a thin-walled open-ended stainless-steel tube containing a gold-plated copper ball that could roll back and fourth in this tube by changing periodically (usually a few times per minute) the inclination of the plate supporting the calorimeter.

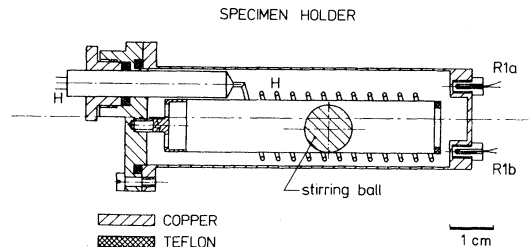


FIG. 1. Specimen holder with stirring system, heater (H) and temperature sensors R_{1a} and R_{1b} .

The thermistor R_{1a} is used in the servosystem controlling the temperature difference with stage 2, and with the thermistor R_{1b} the temperature of the stage 1 can be measured. This sample holder can contain about 25 cm³ of the sample material.

In order to obtain the heat capacity C_s of the sample, three quantities have to be obtained experimentally. The constant electric heating power P_e was obtained from a constant current source with a stability of 0.01%, and calculated from the measured voltages over the heater in the cell and over a standard resistor in series with it. This is the total heating power ($P=P_e$) in case the sample is not stirred. When the sample is also stirred, we have $P=P_e+P_s$ with P_s the stirring power. P_s can be determined from short runs, where P_s is the only power applied to stage 1 and where C_1 is known, e.g., from heat-pulse measurement.⁴⁵ T is found by numerical differentiation from a careful measurement of the temperature (T) versus time (t) evolution of stage 1. The temperature of this stage was measured every 20 sec by means of thermistor R_{1b} of Fig. 1 in a self-balancing six-digit ac potentiometer, giving a temperature resolution of 0.1 mK. Values for $C_h(T)$ are derived from the results of a calibration run with the cell filled with a known amount of water for which accurate specific-heat data are available.⁴⁶

The numerical differentiation, with a subsequent loss of accuracy, which is needed to extract \dot{T} from the $T(t)$ results, can in many cases be avoided. This is certainly the case if information on critical exponents and amplitudes for the pretransitional effects is desired. More directly related to the experimental results are the integral properties

$$\begin{aligned} H_1(T) &= H_1(T_s) + \int_{T_s}^T (C_s + C_h) dT \\ &= H_1(T_s) + P(t - t_s). \end{aligned} \quad (2.2)$$

T_s and t_s refer to the starting conditions of the experiment. The direct experimental results $P(t - t_s)$ and $T(t)$ provide an enthalpy versus temperature curve $H_1(T) - H_1(T_s)$. The relevant theoretical parameters in the specific-heat behavior of the investigated substance are obtained after integration of the theoretical expression for C_s , inserted in Eq. (2.2), and fitting the direct $H_1(T) - H_1(T_s)$ results. If, e.g., the specific-heat behavior above a second-order phase transition at T_c is described by

$$C_p = \frac{A}{\alpha} \epsilon^{-\alpha} + B, \quad (2.3)$$

with $\epsilon \equiv (T - T_c)/T_c$, and if we can identify C_s with C_p , it follows that

$$\begin{aligned} H_1(T) - H_1(T_s) &= \frac{AT_c}{(1-\alpha)\alpha} \left[\left(\frac{T - T_c}{T_c} \right)^{1-\alpha} - \left(\frac{T_s - T_c}{T_c} \right)^{1-\alpha} \right] \\ &\quad + B(T - T_c) + \int_{T_s}^T C_h dT. \end{aligned} \quad (2.4)$$

If one takes the critical temperature T_c and the time it is reached t_c as reference values, for the sample alone one obtains

$$\begin{aligned} H(T) - H(T_c) &= H_1(T) - H_1(T_c) - \int_{T_c}^T C_h dT \\ &= \frac{T_c A}{(1-\alpha)\alpha} \epsilon^{1-\alpha} + BT_c \epsilon. \end{aligned} \quad (2.5)$$

The general behavior of C_p near the transition can be visualized by introducing the quantity

$$\begin{aligned} C(T) &\equiv \frac{P(t - t_c)}{T - T_c} - \frac{1}{(T - T_c)} \int_{T_c}^T C_h(T) dT \\ &= \frac{A}{(1-\alpha)\alpha} \epsilon^{-\alpha} + B, \end{aligned} \quad (2.6)$$

which behaves as C_p in Eq. (2.3) with a $(1-\alpha)^{-1}$ -times-smaller singular part. Similar results for $T < T_c$ and more complex expressions for C_p can be derived (see Sec. IV).

It should be pointed out that Eq. (2.2) is only applicable if no first-order transition occurs between T_s and T . If it were present at a temperature T_{tr} a modified equation would hold:

$$\begin{aligned} H_1(T) - H_1(T_s) &= \int_{T_s}^{T_{tr}} (C_h + C_s) dT + \Delta H_L(T_{tr}) \\ &\quad + \int_{T_{tr}}^T (C_h + C_s) dT. \end{aligned} \quad (2.7)$$

A transformation of the variable temperature T to time t gives

$$\begin{aligned} H_1(T) - H_1(T_s) &= P(t_{tr}^{(i)} - t_s) + P(t_{tr}^{(f)} - t_{tr}^{(i)}) \\ &\quad + P(t - t_{tr}^{(f)}). \end{aligned} \quad (2.8)$$

If thus a latent heat $\Delta H_L(T_{tr})$ occurs, the temperature will be constant for a time interval $t_{tr}^{(f)} - t_{tr}^{(i)} = \Delta H_L/P$. The heating-rate method not only allows us to obtain detailed information on the specific-heat behavior near phase transitions, but it will also give values for the latent heats if present. This is of course of great importance for liquid crystals, where indeed small latent heats have to be distinguished from pretransitional effects.

The 8CB liquid-crystal sample was obtained from BDH Chemicals (product K24 and batch No. 508654) and used as received. The purity stated by

the manufacturer was 99.5% minimum. 21.949 g of 8CB in the isotropic phase (at about 50°C) was transferred into the sample holder. The total heat capacity of the loaded cell was about 85 J/K at 30°C, of which 60% was due to the sample.

III. RESULTS

We have investigated the temperature dependence of the enthalpy and the heat capacity of 8CB in the temperature range between 10 and 50°C. In this temperature range 8CB has three phase transitions. The crystal melts to a smectic-*A* phase at $T_{KA}=22^\circ\text{C}$, it becomes nematic at $T_{AN}=33.8^\circ\text{C}$, and finally isotropic at $T_{NI}=40.8^\circ\text{C}$.

We have carried out several heating runs over limited temperature ranges with special emphasis on the phase transition regions. In Table I a survey for the relevant parameters of the different runs is given. The numbers of the runs are consistent with the chronological sequence in which they have been measured. As is clear from Table I very slow heating rates have been used. Each run took at least a week of constant heating of stage 1 and of data collecting. In addition to the heating runs, a limited number of specific-heat readings were obtained in all three of the phases by means of the conventional heat-pulse method.⁴⁵ The agreement between the heat-pulse data for C_p and the values calculated from the heating runs was within 2%.

In Fig. 2 the general behavior of the heat capacity of 8CB between 10 and 50°C is given. The data points in this figure have been calculated by means of Eq. (2.1) and numerical differentiation of the direct temperature T versus time readings. It is clear from Fig. 2 that all the transitions show pretransitional effects in the specific-heat behavior.

We will now consider the three phase transitions separately in more detail.

A. Crystal to smectic *A*

Two heating runs through the solid to the smectic phase transition have been carried out (see Table I for details). In both cases the sample cell was first cooled to about 0°C to solidify the sample. Both runs were started at about 17°C. A few heat-pulse data have also been taken near 12 and 15°C (see Fig. 2). The results of both runs were essentially the same. In Fig. 3 the enthalpy versus temperature behavior is given. The transition clearly shows a first-order character. The large enthalpy increase between the solid and the smectic-*A* phase does, however, not correspond to a step function; instead an almost linear behavior with a finite slope is observed. This indicates the existence of an impurity broadened two-phase region between about 21.3 and 22°C (see also Fig. 2). Furthermore, a precursor effect clearly occurs in the solid phase between 17 and 21°C. Similar pretransitional effects have been observed²² in the liquid-crystal butyloxybenzylidene-octylaniline (4O.8) for the transition from the normal crystal phase to the plastic crystal *B* phase. Premelting of the hydrocarbon tails and a gradual loss of orientational order around the chain axis might be at the origin of these premelting effects.²²

There is some uncertainty in separating in the $H(T)$ curve the pretransitional effects in the solid phase from the smeared out latent heat contribution in the two-phase region where the solid and the highly viscous smectic-*A* phase coexist. A further complication may arise from inhomogeneities of the impurity concentration in the solid, resulting in a distribution of transition temperature over the sam-

TABLE I. Relevant experimental parameters for the constant heating power runs in 8CB.

Run	T range (°C)	Transition	P (T_s) (10^{-3} W)	dT_1/dt (at T_s) (K/h)	Stirring	Number of T readings
I	32.96–34.50	<i>AN</i>	0.396	0.014	yes	20 580
II	37.59–44.50	<i>NI</i>	1.305	0.050	yes	26 830
III	33.21–34.94	<i>AN</i>	0.735	0.028	no	11 390
IV	34.98–37.11		0.735	0.028	no	8 140
V	37.25–40.75	<i>NI</i>	1.325	0.045	no	13 500
VI	33.14–34.38	<i>AN</i>	0.402	0.015	no	15 400
VII	39.30–49.82	<i>NI</i>	1.686	0.063	yes	29 300
VIII	27.80–33.50		1.323	0.054	no	10 400
IX	17.21–30.72	<i>KA</i>	2.116	0.102	no	72 470
X	17.50–26.19	<i>KA</i>	3.087	0.147	no	43 500

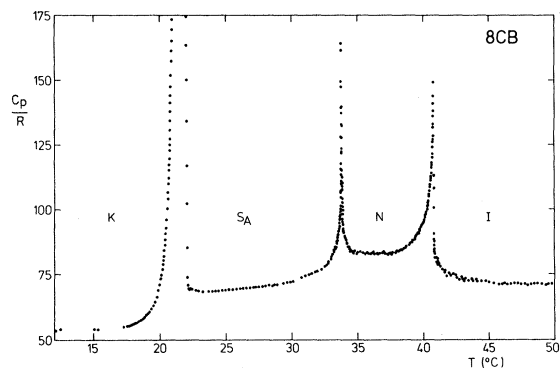


FIG. 2. Reduced heat capacity per mole (R is the gas constant) for octylcyanobiphenyl (8CB) as a function of temperature in the crystalline (K), the smectic- A (S_A), the nematic (N), and the isotropic (I) phases.

ple.³⁹ Finally a certain local metastability cannot be excluded, if one keeps in mind that this system can be undercooled very easily for rather long periods. In order to extract a latent-heat value from the experimental $H(T)$ curve, a careful analysis is thus needed. As already indicated, we estimate the two-phase region to exist between 21.3 and 22.0°C. The end of the two-phase region at 22.0°C (indicated by arrows in Fig. 3) could be rather well determined from the abrupt change in the slope of the $H(T)$ curve (see Figs. 2 and 3). As the initial temperature

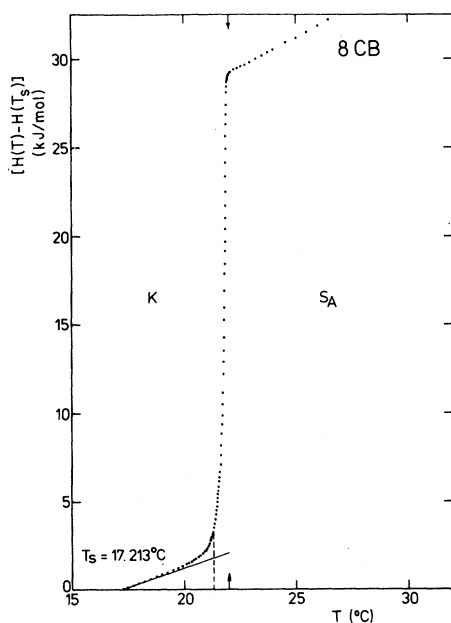


FIG. 3. Temperature dependence of the enthalpy near the solid (K)—to—smectic- A (S_A) phase transition in octylcyanobiphenyl (8CB).

we accepted the temperature where for both runs (IX and X) through this transition an irregular behavior in the first and second temperature derivative of the $H(T)$ curve was noticed. Above that temperature the slope of $H(T)$ reached rapidly very large values. Between 17.2 and 22.0°C, the limiting temperatures of the anomalous region, the total enthalpy increase is 29.1 kJ/mol. The solid line in Fig. 3 corresponds to the enthalpy behavior obtained by integrating an estimated background behavior for the specific heat C_p^B as derived by a linear fit to the C_p data (of Fig. 2) between 10 and 17.5°C. If we now subtract at 21.3°C (indicated by the dashed line in Fig. 3) the enthalpy increase due to this background from the total of 29.1 kJ/mol between 17.2 and 22°C, we arrive at 27.2 kJ/mol. This enthalpy difference still includes the pretransitional increase

$$\delta H = \int (C_p - C_p^B) dT$$

between 17.2 and 21.3°C. From the difference between the solid line and the experimental data points in Fig. 3, a value of $\delta H = 1.5$ kJ/mol is obtained. We arrive thus at a final value of 25.7 ± 1.0 kJ/mol for the latent heat of the KA transition. On the basis of differential scanning calorimetry $\Delta H_{KA} = 25.3$ kJ/mol was obtained by Liebert and Daniels⁴⁷ and $\Delta H_{KA} = 23.4$ kJ/mol was given by Coles and Strazielle.⁴⁸ A value of $\Delta H_{KA} = 25.3$ kJ/mol was also reported by Smith.⁴⁹

B. Smectic A to nematic

For this phase transition we have carried out three runs (runs I, III, and VI of Table I). During run I the sample was also stirred in the way described in Sec. II. The stirring power was experimentally determined from several short runs in which the stirring was the only source of heat of the sample, and where C_p values were known from heat-pulse measurements. The heat input at constant stirring rate turned out to be temperature dependent in the S_A phase but almost constant in the nematic as well as in the isotropic phase. This suggests that the viscosity of the fluid plays an important role in the energy conversion. The stirring power was about 8% of the total power for run I and less than 2.5% for runs II and VII. Two other runs without stirring and with heating rates which differed by about a factor of 2 were also carried out for the AN transition.

In Fig. 4(a) the enthalpy versus temperature curve for run VI is given in and Fig. 4(b), the correspond-

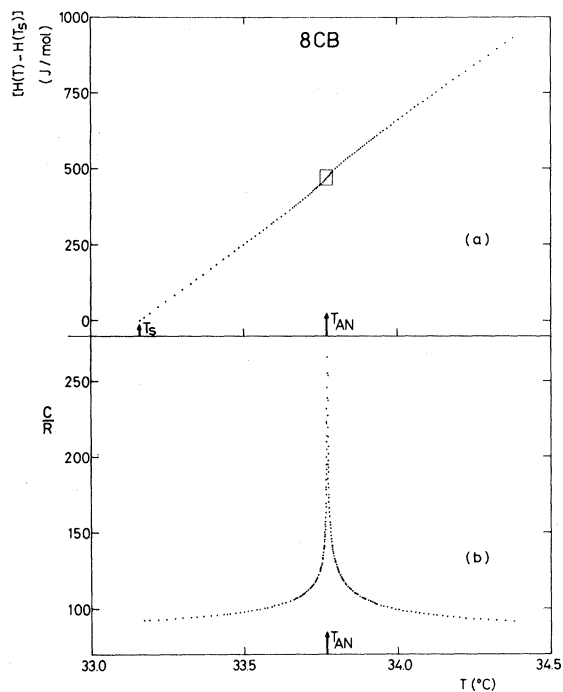


FIG. 4. (a) Enthalpy change $H(T) - H(T_s)$ near the smectic- A to-nematic (AN) phase transition in 8CB as a function of temperature, for a constant heating power run with T_s as starting temperature. (b) Temperature dependence of the reduced quantity C per mole defined in Eq. (2.6) and calculated from the data given in (a).

ing values for the experimental quantity C , defined in Eq. (2.6). The enthalpy curve in Fig. 4(a) does not reveal any discontinuous latent heat increase at the T_{AN} transition temperature. This remains the case if one takes a closer look at the immediate vicinity of the transition in Fig. 5, which is a blow up of the small square in Fig. 4(a). Within the resolution of our experiment there is no evidence for a latent heat at the AN transition. From the data in Fig. 5 and from the two other runs (I and III) we arrive at an upper limit of 0.4 J/mol or 1.4×10^{-3} J/g for the latent heat. In fact, our data for AN suggest a continuous second-order phase transition. Our conclusion on the latent heat is in disagreement with some earlier statements. Therefore we will discuss it in more detail.

Let us first point out that the absence of a latent heat for the AN transition is not in contradiction with the theoretical models by de Gennes³ or by McMillan² and Kobayashi,¹ where it was obtained that this transition can be either first or second order. Our experimental result lends support to the

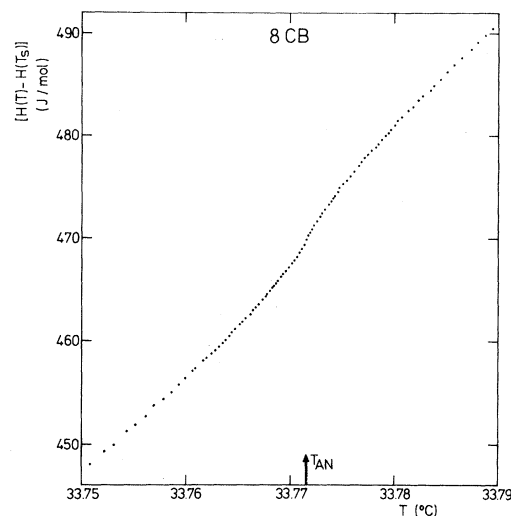


FIG. 5. Enthalpy change $H(T) - H(T_s)$ as a function of temperature in a very narrow temperature range around the smectic- A to-nematic (AN) phase transition in 8CB. This figure is a blow up of the small square in Fig. 4(a).

recent theoretical conclusions on this matter by Dasgupta and Halperin,⁸ Helfrich,⁹ and Nelson and Toner.¹⁰ If a latent heat is present it must be very small; at least a thousand times smaller than the latent heat for the NI transition (see Sec. III C) and 10^5 times smaller than the heat of fusion.

As a further point of discussion we now treat the compatibility of our data with those of other thermodynamic studies. A most interesting comparison can be made with results obtained in the same system by means of differential scanning calorimetry (DSC). Widely differing latent heat values of 126, 42, 130, and 200 J/mol have been published.⁴⁷⁻⁵⁰ The apparent conflict with our result is probably due largely to a confusion between the meaning of a true latent heat, which should be related to a purely first-order transition, and that of heat of transition which may also include, besides a latent heat, pretransitional effects. It has already been pointed out by Kasting *et al.*^{19,20} that DSC data obtained with the conventional scanning rates, typically between 0.5 and 5 K/min (this is more than 10^3 times faster than in our experiment), will show rounding-off effects and thermal relaxation effects. This makes it almost impossible to distinguish, on the experimental DSC curves, between different contributions in the total heat of transition. Kasting *et al.*,²⁰ in interpreting their ac heat-capacity data, estimated the total enthalpy change due to pretransitional effects by calculating

$$\delta H_{AN} = \int \Delta C_p dT$$

with $\Delta C_p = C_p(T) - C_p^B(T)$, where $C_p^B(T)$ represents an hypothetical baseline behavior of C_p in the absence of the second-order contribution. They obtain $\delta H_{AN} = 228$ J/mol for the AN transition in 8CB. From our data we obtain, with as baseline a linear behavior between the C_p values at 31 and 37°C, a total enthalpy increase $\delta H_{AN} = 218$ J/mol. Both δH_{AN} values are in good agreement. The DSC result⁵⁰ of 200 J/mol, if interpreted as entirely due to pretransitional enthalpy changes, is also close to the above δH_{AN} values.

From density measurements^{50,51} in 8CB, it was concluded that the AN transition showed a discontinuous first-order jump in that quantity. Leadbetter *et al.*⁵⁰ reported a discontinuous volume change $\Delta V = 0.14 \pm 0.04$ cm³/mol (or $\Delta V/V = 4.7 \times 10^{-4}$) and Dunmur and Miller⁵¹ give $\Delta V/V = 3 \times 10^{-4}$. First-order volume changes can be related to corresponding latent heats via the Clapeyron-Clausius relation

$$\Delta V = T \Delta V \frac{dp}{dT_{AN}}. \quad (3.1)$$

Using this equation and our upper limit for a possible latent heat $\Delta H_{\max} = 0.4$ J/mol, we can derive a corresponding upper limit ΔV_{\max} , provided dp/dT_{AN} is known. From the phase diagram of 8CB obtained by Kasting *et al.*,²⁰ we arrive at $dp/dT_{AN} \simeq 46$ bar/K. As the upper limit for a possible discontinuity in the molar volume, we arrive then at $\Delta V_{\max} = 2.8 \times 10^{-4}$ cm³/mol. This is more than two orders of magnitude smaller than the ΔV values given in Refs. 50 and 51. This discrepancy is most likely the result of the limited temperature stability (± 0.02 K) and an unjustified extrapolation procedure of the density data to T_{AN} . As it is the case for the transitional enthalpy change (see Fig. 5), much of the continuous volume change must occur in a very narrow temperature range of a few hundredths of a degree around T_{AN} . In analogy with the DSC case, the ΔV values of Leadbetter *et al.*⁵⁰ and of Dunmur and Miller⁵¹ should probably also be interpreted as pretransitional volume changes δV_{AN} .

From the behavior of the quantity C in Fig. 4(b) it is clear that the specific heat in both phases near the AN transition has a quite large anomalous behavior, which can presumably be described by power laws. This aspect will be discussed in Sec. IV. In Fig. 6 a comparison is made between the direct C_p results obtained by Kasting *et al.*^{20,52} with an ac technique, and values calculated from our

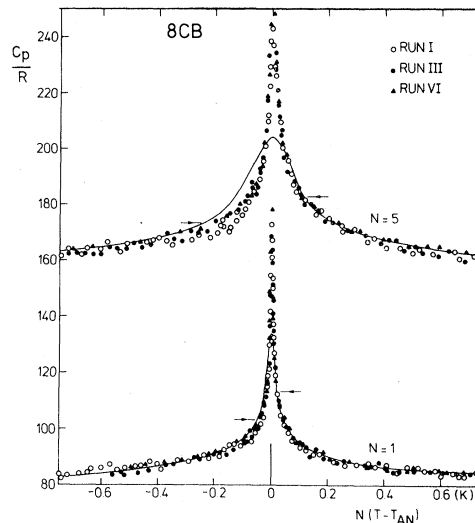


FIG. 6. Reduced heat capacity per mole calculated by means of Eq. (2.1) from three constant heating power runs (see Table I) through the smectic- A to -nematic (AN) phase transition in octyloxybiphenyl (8CB). The solid line represents ac-calorimetric data obtained by Kasting, Garland, and Lushington (Ref. 20). In addition to the indicated enlargement of the temperature scale, a value of 70 has been added to the C_p/R values in the top part of the figure.

three heating runs by means of Eq. (2.1) and numerical differentiation of the $T(t)$ readings. Note that T_{AN} , which corresponds to the temperature of the C_p maximum, was 0.230 K lower in Ref. 20 than the value we observed. In the upper part of the figure the temperature scale was enlarged by a factor of 5. For both representations there is good agreement between the results of our three runs. Only some data of run I in the S_A phase close to T_{AN} fall on the average a little bit below the two other runs. This is most likely caused by the somewhat larger uncertainty on the stirring power in that range. The transition temperatures for our three runs do not differ more than 2 mK. This is a very good reproducibility if one realizes that between run I and VI there was a time lapse of more than a year. The solid lines in Fig. 6 represent the ac results.²⁰ For most of the data there is very good agreement with our adiabatic results. However, the ac data show a rounding-off effect near T_{AN} . The authors of Ref. 20 were aware of this effect, which they ascribed to impurities, and data closer to T_{NA} than the values indicated by the arrows were not used in their fits.⁵³ Data in a pure 8OCB sample, also measured with an ac technique by the same authors, did not show any rounding effect.¹⁹

C. Nematic to isotropic

Three different runs (runs II, V and VII of Table I) have been carried out for the nematic-to-isotropic transition. In Fig. 7 parts of the $H(T)$ curve from runs II and VII are given. For display reasons there is a shift of 20 mK between the temperature scales of both runs. The width and the temperatures of the very small two-phase region do not differ by more than 2 mK. Here, also, the time lapse between the two runs was more than a year. The observed NI transition clearly shows a first-order character with a latent heat $\Delta H_{\text{NI}}=612(\pm 5)$ J/mol. It is also only very slightly (14 mK) impurity broadened. This rather small two-phase region is an indication of good purity of the sample. In Fig. 7 it can be observed that the transition from the two-phase region to the isotropic phase is much more rounded than between the two-phase region and the nematic phase. We ascribe this rounding off to the persistence of long thermal relaxation times for that region. It can also be observed that the rounding-off effect is somewhat less pronounced for run II than for run VII, which was measured at a 30% faster heating rate. We had also seen much more rounding of the $H(T)$ curve for the same range in a series of preliminary runs with much faster heating rate or without stirring.

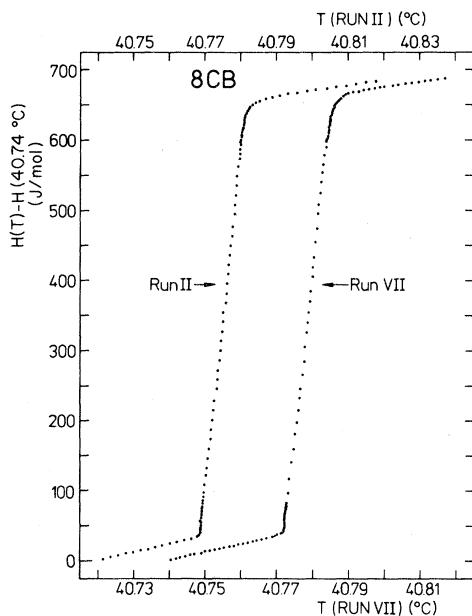


FIG. 7. Temperature dependence of the enthalpy near the nematic-to-isotropic (NI) phase transition in octylcyanobiphenyl (8CB) as obtained from two different heating runs (see Table I).

Several ΔH values for this transition are available from DSC measurements: Liebert and Daniels⁴⁷ obtained 879 J/mol; Coles and Strazielle,⁴⁸ 670 J/mol; Leadbetter *et al.*,⁵⁰ 700 J/mol; and Smith,⁴⁹ 971 ± 80 J/mol. These values are larger than the value we obtained on the basis of the results in Fig. 7. The remarks on the reliability of the DSC results near the AN transition also apply here. It is quite certain that DSC latent-heat values contain part of the pretransitional enthalpy change. Leadbetter *et al.*⁵⁰ reported for the NI transition a volume change $\Delta V=0.95 \pm 0.15$ cm³/mol (i.e., $\Delta V/V=33 \times 10^{-4}$), Dunmur and Miller⁵¹ give $\Delta V/V=17 \times 10^{-4}$. We can use Eq. (3.1) to convert these volume changes into latent heats. From the phase diagram²⁰ of 8CB we obtain $dp/dT_{\text{NI}} \approx 31$ bar/K. The above volume changes would thus correspond with $\Delta H_{\text{NI}}=930 \pm 150$ J/mol and $\Delta H_{\text{NI}}=490$ J/mol.

The pretransitional effects near T_{NI} are looked at in Fig. 8, where C_p values for the immediate vicinity of the NI transition are given. The C_p values are again calculated with Eq. (2.1) and numerical differentiation of the direct $T(t)$ data. The results for the different runs are in very close agreement. A comparison is also made with the ac results of Kasting *et al.*²⁰ We have increased the temperature of the ac results by 0.310 K in order to shift the maximum of $C_p(\text{ac})$ to coincide with that in our data. Apart from a small overall shift in absolute value, a substantial difference in the isotropic phase just above the transition is observed. A clear explanation for this discrepancy is not available. It should, however, be noted that for temperatures just

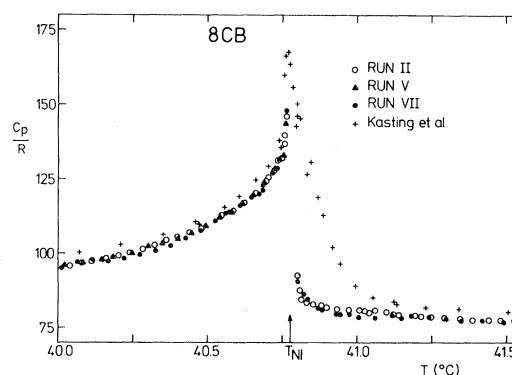


FIG. 8. Reduced heat capacity per mole calculated by means of Eq. (2.1) from three different constant heating power runs (see Table I) through the nematic-to-isotropic (NI) phase transition of octylcyanobiphenyl (8CB). A comparison is also made with the ac results by Kasting *et al.* (Ref. 20).

above T_{NI} , C_p values calculated from our preliminary runs with faster rates or without stirring also fell above our equilibrium values (in Fig. 8), measured at much lower heating rates and with stirring.

IV. ANALYSIS AND DISCUSSION

A. Equations and fitting procedure

Theoretical predictions about second-order phase transitions result in power-law expressions for the asymptotic behavior of certain properties at the critical point. Different universality classes are characterized by different sets of critical exponent values (see, e.g., Ref. 4). The theoretical predictions for the heat capacity C_p are summarized in the following expressions:

$$C_p = \frac{A}{\alpha} \epsilon^{-\alpha} (1 + D\epsilon^\Delta + \dots) + B + E\epsilon, \quad (4.1a)$$

with $\epsilon \equiv (T - T_c)/T_c$ for $T > T_c$, and

$$C_p = \frac{A'}{\alpha'} \epsilon'^{-\alpha'} (1 + D'\epsilon'^{\Delta'} + \dots) + B' + E'\epsilon', \quad (4.1b)$$

with $\epsilon' \equiv (T_c - T)/T_c$ for $T < T_c$. The leading contributions to the heat capacity singularity are given by $(A/\alpha)\epsilon^{-\alpha}$ and $(A'/\alpha')\epsilon'^{-\alpha'}$. The factors $(1 + D\epsilon^\Delta + \dots)$ and $(1 + D'\epsilon'^{\Delta'} + \dots)$ represent correction to scaling.⁵⁴ The last two terms account for the constant critical contribution and the regular background behavior of the heat capacity. Sufficiently close to the critical point it is expected that the contribution from the correction to scaling terms, and from the temperature dependence of the background, can be neglected, and one obtains the asymptotic form given in Eq. (2.3). Integrating Eq. (4.1a) results in the following expression for the enthalpy difference ΔH and for the quantity C defined in Eq. (2.6):

$$\begin{aligned} \Delta H &= H(T) - H(T_c) \\ &= \frac{AT_c}{\alpha(1-\alpha)} \epsilon^{1-\alpha} \left[1 - \frac{D(1-\alpha)}{1+\Delta-\alpha} \epsilon^\Delta \right] \\ &\quad + BT_c \epsilon + \frac{ET_c}{2} \epsilon^2, \end{aligned} \quad (4.2)$$

$$\begin{aligned} C &= \frac{A}{\alpha(1-\alpha)} \epsilon^{-\alpha} \left[1 + \frac{D(1-\alpha)}{1+\Delta-\alpha} \epsilon^\Delta \right] \\ &\quad + B + \frac{E\epsilon}{2}. \end{aligned} \quad (4.3)$$

From Eq. (4.1b) for $T < T_c$, identical results as in Eqs. (4.2) and (4.3) are obtained but with corresponding primed symbols.

In the analyses of the data we carried out several nonlinear least-squares fits⁵⁵ for the quantity ΔH in Eq. (4.2). To obtain the best parameter values, the chi-square function

$$\chi^2 = \sum_{j=1}^n \frac{(\Delta H_{\text{expt}}^j - \Delta H_{\text{calc}}^j)^2}{\text{var}(\Delta H^j)} \quad (4.4)$$

was minimized for n data points. The variance is given by

$$\begin{aligned} \text{var}(\Delta H^j) &= (\sigma_H^j)^2 + (C_p^j)^2 (\sigma_T^j)^2 \\ &\simeq (\sigma_H^j)^2 + C_j^2 (\sigma_T^j)^2, \end{aligned} \quad (4.5)$$

with C_j the quantity defined in Eq. (2.6). The first term results from the overall scatter on the $H(T)$ data readings and the second one accounts for the increasing importance, on approaching T_c , of the uncertainty of a temperature reading. Since a data point was taken every 20 sec, a very large number of data points was obtained for each run (see Table I). It was not feasible to fit these results directly with the minimization program. Instead N_j direct data were properly averaged. N_j ranged from 5 to 150 depending on the rate of the run and the distance from the transition. This resulted in a few hundred "data points" for each run that were actually used for the minimization of χ^2 of Eq. (4.4).

B. Fits for the AN transition

Following the above-described procedure, we have carried out several fits for the three runs (see Table I) through the AN transition, with the purpose of extracting values for the critical exponents α and α' and for the amplitudes A and A' . Before discussing the fitting results, we first want to give some important qualitative information on these parameters, which can be deduced directly from the data without the minimization procedure.

In Fig. 9, we have plotted on a double-logarithmic scale the C values for runs III and VI, as well as the C_p values from run VI and from the ac measurements of Kasting *et al.*²⁰ It is quite clear that for the whole range of the reduced temperature difference $|\epsilon|$ covered in Fig. 9, the C_p values fall systematically below the C values. Furthermore, $C - C_p$ substantially increases on approaching T_{AN} . This can be clearly seen in Fig. 10, where $C - C_p$ versus $|\epsilon|$ is plotted on a double-logarithmic scale. The value for T_{AN} was deter-

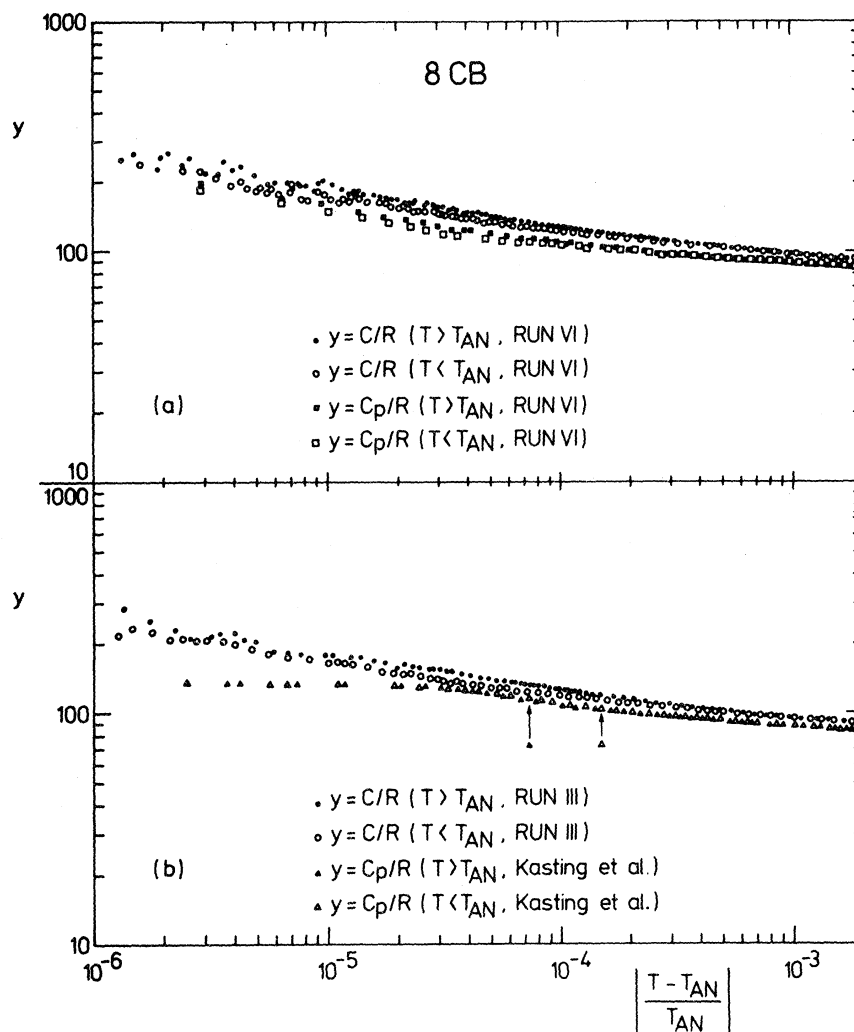


FIG. 9. Comparisons on a double-logarithmic scale of the quantities C_p/R and C/R as a function of the reduced temperature difference with the smectic-A-to-nematic phase transition temperature (T_{AN}) in octylcyanobiphenyl (8CB). C_p is the heat capacity per mole, C is the quantity defined in Eq. (2.6) per mole, and R is the gas constant. Data of Kasting *et al.* (Ref. 20) to the left of the arrows show rounding-off effects and have not been used by these authors in the power-law analysis.

mined from a careful inspection of the direct $H(T)$ data close to $T_c = T_{AN}$. A value $T_{AN} = 33.7716 \pm 0.0003^\circ\text{C}$ was obtained for run VI. According to Eqs. (4.1a) and (4.3) one finds

$$C - C_p = \frac{A}{1 - \alpha} \epsilon^{-\alpha} \left[1 + D \epsilon^\Delta \left(1 - \frac{\Delta}{\alpha(1 + \Delta - \alpha)} \right) \right] - \frac{E}{2} \epsilon \quad (4.6)$$

for $T > T_c$, and an identical result with primed symbols for $T < T_c$. This way of presenting the data has the great advantage that the adjustable

parameter B is eliminated and that in double-logarithmic plot a linear relationship is found in the ϵ range where higher-order terms can be neglected. Figure 10 shows the $C - C_p$ results above and below T_{AN} . Linear fits to the data for $\epsilon < 10^{-3}$ give identical slopes $\alpha = \alpha' = 0.316$ and an amplitude ratio $A'/A = 0.82$.

In order to verify the above conclusions, a series of nonlinear least-squares fits have also been carried out for the direct experimental ΔH results by means of Eq. (4.2). In a first series of fits we analyzed the data above and below $T_c = T_{AN}$ separately. For most of the fits we used the asymptotic form (2.5),

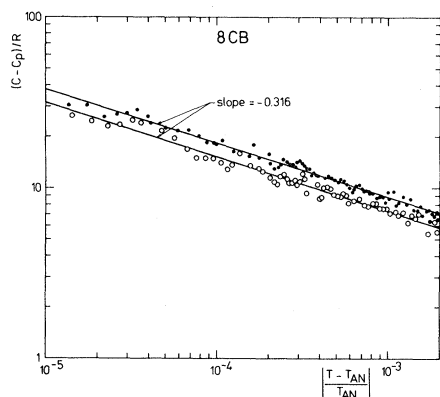


FIG. 10. Double-logarithmic plot of $C - C_p/R$ vs the reduced temperature difference with the smectic- A to-nematic phase transition temperature (T_{AN}) in octylcyanobiphenyl (8CB). C and C_p are, respectively, the quantity defined in Eq. (2.6) and the heat capacity per mole. Results in this figure are from run VI [see also Fig. 4(a)]. Open symbols are for the smectic- A phase and solids for the nematic phase.

which is appropriate in the range where correction terms are unimportant. This can be verified by the procedure of range shrinking. We have applied it to our data. In Table II the parameter values for the different fits are given. In the second column of the table the fitted data are identified by the run (see Table I) and the phase symbol N (for $T > T_{AN}$) or A (for $T < T_{AN}$). In the last column of Table II we have also given the reduced chi-square function

$$\chi_v^2 = \chi^2 / (n - p), \quad (4.7)$$

which is a measure for the quality of the fits. In Eq. (4.7), χ^2 is the expression given in Eq. (4.4), n is the number of data points, and p is the number of adjustable parameters in the fit. For the different fits the uncertainty on each parameter is not explicitly quoted. For one standard deviation, however, the uncertainty in the parameters is usually less than a few units in the last digit. It should also be noted that the values for $H_c - H_s$, which are needed in the fits, do not have a special physical relevance, since the starting point of a run is arbitrary. The transition temperature T_c and $H_c - H_s$ were held constant in fits 1–12 and 17–26 at the best values deduced from the direct $H(T)$ results. Some fits with slightly different T_c and $H_c - H_s$ values, reflecting the experimental uncertainty, have also been done. The effect of range shrinking was investigated by carrying out the analyses for different $|\epsilon|_{\max}$ values between 2×10^{-3} and 3×10^{-4} . $|\epsilon|_{\min}$ was held constant at a value of 1.5×10^{-6}

for $T < T_{AN}$ and 1.3×10^{-6} for $T > T_{AN}$. For the data below T_c (fits 1–4) there is no evidence of a systematic range dependence on the parameters. In the nematic phase above T_c (fits 5–8) a small range dependence on α is observed for fits with $|\epsilon|_{\max} > 6 \times 10^{-4}$. The results of fits 1–8 are qualitatively confirmed by the fits 9–12 where it can be seen that below T_c the correction terms do not substantially improve the fits or change the parameter values. Above T_c for large $|\epsilon|_{\max}$ values an improvement can be obtained with correction terms, and also an α value closer to the ones in fits 7 and 8 is obtained. For the correction to scaling exponent Δ in fits 10 and 12 a value of 0.5 was imposed. This value for Δ is consistent with theoretical estimates.⁴ The uncertainty in T_c and $H_c - H_s$ is investigated in fits 13–16. Changes of the order of 10% in α or α' are obtained. The fits are, however, not as good and the effect of the same shift in T_c and $H_c - H_s$ results in opposite changes in α and α' . Our most reliable T_c and $H_c - H_s$ values are consistent with $\alpha = \alpha'$, but this is not the case for the other choices investigated. Fits 1–16 have been carried out for the data of run VI. In lines 17 and 18 fits for run III are also given, resulting in α and α' values in agreement with those obtained for run VI. It should also be pointed out that there is no indication of crossover to a different α value for the data very close to the transition point. This can be verified in Fig. 11, where deviation plots for the fits

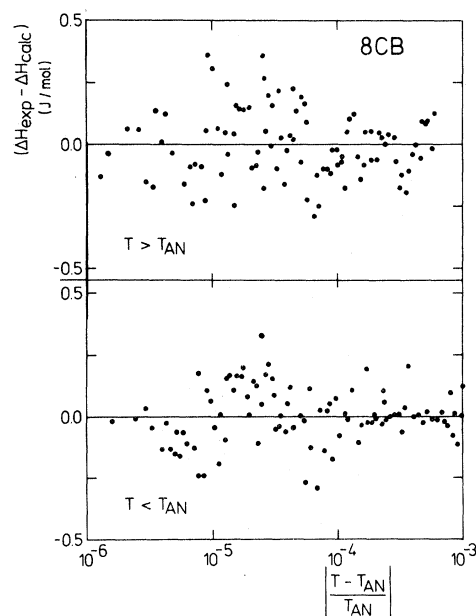


FIG. 11. Deviation plots for the fits 2 and 7 of Table II to the direct enthalpy data of run VI with Eq. (4.2).

TABLE II. Parameter values from separate fits to the data above the smectic-A - to - nematic phase transition ($T_c \equiv T_{AN}$) with Eq. (4.2) and with an identical equation with primed symbols for the data below T_{AN} .

Fit	Run phase	α, α'	A, A' _a	B, B' _a	D, D'	Δ, Δ'	E, E' _a	T_c, T'_c (°C)	$H_c - H_s$ (J/mol)	$ \epsilon _{\max}$	χ^2_c
1	VI-A	0.295	0.691	71.7				(33.7716) ^b	(469.97)	2×10^{-3}	1.936
2	VI-A	0.305	0.627	72.9				(33.7716)	(469.97)	1×10^{-3}	1.888
3	VI-A	0.306	0.622	73.0				(33.7716)	(469.97)	6×10^{-4}	2.003
4	VI-A	0.316	0.555	74.7				(33.7716)	(469.97)	3×10^{-4}	2.150
5	VI-N	0.341	0.538	71.7				(33.7716)	(469.97)	2×10^{-3}	2.778
6	VI-N	0.320	0.665	69.0				(33.7716)	(469.97)	1×10^{-3}	2.097
7	VI-N	0.294	0.866	64.7				(33.7716)	(469.97)	6×10^{-4}	2.178
8	VI-N	0.294	0.878	64.2				(33.7716)	(469.97)	3×10^{-4}	2.150
9	VI-A	0.310	0.595	73.7			-3.7×10^2	(33.7716)	(469.97)	2×10^{-3}	1.827
10	VI-A	0.305	0.630	72.0	2.2	(0.5)	-4.7×10^2	(33.7716)	(469.97)	2×10^{-3}	1.844
11	VI-N	0.305	0.812	64.8			1.5×10^3	(33.7716)	(469.97)	2×10^{-3}	2.684
12	VI-N	0.319	0.675	69.1	-1.3	(0.5)	8.7×10^2	(33.7716)	(469.97)	2×10^{-3}	2.156
13	VI-A	0.269	0.842	69.6				(33.7713)	(469.39)	1×10^{-3}	2.019
14	VI-A	0.342	0.456	75.7				(33.7719)	(470.60)	1×10^{-3}	1.945
15	VI-N	0.341	0.560	70.7				(33.7713)	(469.39)	1×10^{-3}	2.033
16	VI-N	0.291	0.841	66.3				(33.7719)	(470.60)	1×10^{-3}	2.448
17	III-N	0.300	0.842	63.8				(33.7699)	(984.74)	1×10^{-3}	4.031
18	III-A	0.285	0.739	69.5				(33.7699)	(984.74)	1×10^{-3}	1.851
19	III-A	(0.50)	0.088	84.9				(33.7699)	(984.74)	1×10^{-3}	40.766
20	III-A	(0.11)	3.73	13.6				(33.7699)	(984.74)	1×10^{-3}	20.370
21	VI-A	(-0.02)	11.8	604.1				(33.7716)	(469.97)	1×10^{-3}	71.149
22	VI-A	(-0.02)	22.2	1020.1	-1.25	(0.5)		(33.7716)	(469.97)	1×10^{-3}	9.608
23	VI-A	(-0.02)	58.4	2231.1	-0.32	(0.1)		(33.7716)	(469.97)	1×10^{-3}	4.623
24	VI-N	(-0.02)	17.5	838.4				(33.7716)	(469.97)	6×10^{-4}	49.748
25	VI-N	(-0.02)	32.8	1450.3	-1.65	(0.5)		(33.7716)	(469.97)	6×10^{-4}	5.676
26	VI-N	(-0.02)	86.5	3224.4	-0.34	(0.1)		(33.7716)	(469.97)	6×10^{-4}	2.991

^aIn molar units divided by the gas constant R .

^bParameter values between parentheses indicate that the parameter was held constant at the quoted value.

2 and 7 of Table II are given. For run III we also investigated the compatibility of $\alpha = \alpha' = 0.50$ and $\alpha = \alpha' = 0.11$ with the data. In lines 19 and 20 of Table II only the results for the smectic-*A* phase are given, but similar results were obtained for the nematic phase. It can be concluded that a tricritical value (0.50) and a $d = 3$ Ising value (0.11) are not compatible with the experimental results, since imposing these α values resulted in poor fits with large χ_v^2 values and large systematic deviations. The compatibility of the data with an *XY* value ($\alpha = \alpha' = -0.02$) for the critical exponent has been investigated in fits 21–26 of Table II. The χ_v^2 values in the fits 21 and 24 indicate that in this case a simple power law plus a constant background term results in very poor fits. Lower χ_v^2 values can be obtained if a correction to scaling term is introduced in the fitting equation (4.2). However, the theoretically⁴ expected value

$$\Delta = \Delta' = 0.50 \pm 0.02$$

for the *XY* model still gives very unsatisfactory fits (lines 22 and 25 of Table II). Only for rather small (< 0.2) Δ values, as, e.g., for $\Delta = 0.1$ in the fits 23 and 26 of Table II, reasonably low χ_v^2 values are obtained. It should, however, be noted that large compensating effects are observed with large correction-term contributions also very close to the transition point; e.g., in the case of the fits 23 and 26 the correction term still accounts for about 10% of the singular part of the heat capacity at $|\epsilon| = 10^{-6}$.

In a second series of fits the data above and below T_c have been analyzed simultaneously. In the fits the conditions $T_c = T'_c$, $H_c = H'_c$, and also the scaling relation $\alpha = \alpha'$ have been imposed. For most cases a smooth background behavior was imposed by the constraints $B = B'$ and $E = -E'$. Table III summarizes these results. In fits 1–3 with four adjustable parameters $\alpha = \alpha'$, A , A' , and $B = B'$, range shrinking has been applied to the data of run VI. It is only for the case $|\epsilon|_{\max} = 3 \times 10^{-4}$ that a reasonably low χ_v^2 value is obtained under these conditions. In fits 4 and 5 the effect of additional terms in Eq. (4.2) for $|\epsilon|_{\max} = 2 \times 10^{-3}$ are investigated. For the corrections to scaling exponent Δ we also imposed a value of 0.5. Only in fit 5, where three additional adjustable parameters have been introduced, is a good χ_v^2 value obtained. Very good fits can, however, also be obtained with only five adjustable parameters, by relaxing the constraint $B = B'$. This can be verified in lines 6–8 in Table III. The observed differences in B and B' are

of the same order of magnitude here as for the separate fits 1–8 of Table II. This picture is confirmed by the parameter values in lines 9–12 of Table III for fits to the data of runs III and I. It is clear from the Table III that, unless additional adjustable parameters are introduced, the data, even for $|\epsilon|_{\max} < 3 \times 10^{-4}$, cannot be well fitted with the constraint $B = B'$ imposed. The physical meaning of the values for the correction-term parameters seems to be questionable because sign changes and compensation effects on other parameters do occur. The value for $\alpha = \alpha'$, however, is rather insensitive to the introduction of additional parameters in the fits, and is in very good agreement with the α and α' results of the separate fits in Table II. It can be also observed that, for the fits with small enough χ_v^2 value, a stable value $A'/A \simeq 0.8$ is obtained. These values for α, α' and A'/A from the fitting procedure are in good agreement with the results based on the $C - C_p$ data in Fig. 10. On the basis of this agreement and on the reliable fits in Tables II and III, we arrive at the following best values:

$$\begin{aligned} \alpha = \alpha' &= 0.31 \pm 0.03, \\ A'/A &= 0.83 \pm 0.05. \end{aligned} \quad (4.8)$$

We now compare the results in (4.8) with other experimental values and with theoretical predictions for these quantities. In Table IV we have summarized the available experimental information for the *AN* transition in 8CB. There is quite good agreement, around $\alpha \simeq 0.3$, between the experimental values from four different sources. Our experimental value $\alpha = 0.31 \pm 0.03$ is also in very good agreement with the value we can calculate with Eq. (1.2) from correlation-length exponent values. Litster *et al.*²⁶ obtained for 8CB, $\nu_{||} = 0.67 \pm 0.03$ and $\nu_{\perp} = 0.51 \pm 0.03$. We thus obtain

$$\alpha = 2 - (2\nu_{\perp} + \nu_{||}) = 0.31 \pm 0.09. \quad (4.9)$$

A summary of the available experimental values for the critical exponents α and α' for the *AN* transition in different systems is given in Fig. 12 as a function of T_{AN}/T_{NI} . We did not distinguish between α and α' because good fits to the experimental data could be obtained with $\alpha = \alpha'$ imposed, although in some cases this required correction terms in the fit equations.²⁷ The error bars in Fig. 12 correspond to the values quoted by the authors in the appropriate references. All the values for α in Fig. 12 have been obtained by ac calorimetry, except our result and the one by Djurek *et al.*,⁵⁶ who derived the specific heat from the thermal response curve after a step-function heat input to the sample and

TABLE III. Parameter values from simultaneous fits to the data above and below the smectic-A to -nematic phase transition ($T_c = T_{AN}$) with Eq. (4.2) for $T > T_c$ and an identical one with primed symbols for $T < T_c$.

Fit	Run	$\alpha = \alpha'$	A _a	A'/A	B, B' _a	D, D' _b	$E = -E'$ _a	$T_c = T'_c$	$H_c - H'_s$ (J/mol)	$ \epsilon _{\max}$	χ^2_v
1	VI	0.329	0.560	0.97	72.8			(33.7716) ^c	(469.97)	1×10^{-3}	25.237
2	VI	0.324	0.600	0.95	72.0			(33.7716)	(469.97)	6×10^{-4}	11.824
3	VI	0.329	0.570	0.92	73.4			(33.7716)	(469.97)	3×10^{-4}	4.705
4	VI	0.325	0.589	0.95	72.2		-9.3×10^2	(33.7716)	(469.97)	2×10^{-3}	14.731
5	VI	0.314	0.704	0.85	69.6	$-3.4(D)$ $8.9(D')$	1.2×10^3	(33.7716)	(469.97)	2×10^{-3}	2.119
6	VI	0.323	0.637	0.85	70.0(B) 74.1(B')			(33.7716)	(469.97)	2×10^{-3}	3.898
7	VI	0.307	0.762	0.81	66.8(B) 73.2(B')			(33.7716)	(469.97)	6×10^{-4}	2.027
8	VI	0.309	0.738	0.83	67.5(B) 73.1(B')			(33.7718)	(470.26)	6×10^{-4}	2.007
9	III	0.330	0.575	0.94	71.0			(33.7699)	(984.74)	1×10^{-3}	42.284
10	III	0.333	0.564	0.76	80.4	$23.5(D)$ $-10.0(D')$	1.6×10^3	(33.7699)	(984.74)	1×10^{-3}	3.297
11	III	0.295	0.886	0.76	62.9(B) 70.7(B')			(33.7699)	(984.74)	1×10^{-3}	2.980
12	I	0.288	0.907	0.63	62.3 74.9			(33.7705)	(657.07)	1×10^{-3}	4.976

^aIn molar units divided by the gas constant R .

^bWith the exponent $\Delta = 0.5$.

^cParameter values between parentheses indicate that the parameter was held constant at the quoted value.

TABLE IV. Relevant parameter values from different sources for the heat capacity anomaly of the smectic-*A*—to—nematic phase transition in 8CB.

Source	T_{AN} (K)	$\alpha = \alpha'$	A'/A
Kasting, Garland and Lushington ^a	306.690	0.30 ± 0.05	1.08
LeGrange and Mochel ^b	307.017	0.285 ± 0.03	1.03
Hatta and Nakayama ^c	306.598	0.25 ± 0.02	
This work	306.921	0.31 ± 0.03	0.83 ± 0.05

^aReference 20.

^bReference 24.

^cReference 25.

the sample holder. For several systems there seems to be a rather broad spectrum of α values reported. This is in particular the case for another extensively studied cyanobiphenyl (8OCB), where conflicting

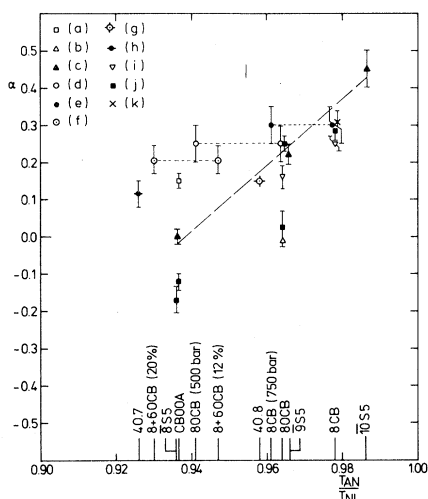


FIG. 12. Survey of the experimental values for the critical exponent α reported in the literature for the smectic-*A*—to—nematic phase transition in different liquid crystals. α values are plotted as a function of the ratio of the smectic-*A*—nematic phase transition temperature T_{AN} to the nematic-isotropic phase transition temperature T_{NI} . For the meaning of the abbreviations used for the different liquid crystals we refer to the text or to the appropriate references. Dashed line connects results (solid triangles) for three materials of the same $\bar{8}S5$ homologous series. Dotted lines connect α values for the *AN* transition in the same material, but where T_{AN}/T_{NI} was changed by applying pressure or adding another component of the same homologous series. Origin of the α values is as follows: (a) Ref. 56; (b) Ref. 15; (c) Refs. 16 and 17; (d) Refs. 18 and 19; (e) Ref. 20; (f) Ref. 21; (g) Refs. 22 and 28; (h) Ref. 23; (i) Ref. 25; (j) Ref. 24; (k) this work.

results have been reported. The discrepancies have been ascribed to impurity effects.^{20,24,27} The first result by Johnson *et al.*¹⁵ was consistent with the *XY* value $\alpha = -0.02$. Some problems, however, occurred for the data close to the transition, where an impurity broadened two-phase region was reported. Subsequent ac results on a different 8OCB sample by Garland *et al.*^{18,19} did not show this effect and resulted in a much larger $\alpha \approx 0.25$ value. Measurements by Hatta and Nakayama²⁵ on 8OCB, resulted in $\alpha = 0.16 \pm 0.03$. LeGrange and Mochel²⁴ remeasured two different 8OCB samples, one with the same origin as the sample of Johnson *et al.*¹⁵ and another one from the same batch as the sample of Garland *et al.*^{18,19} They obtained two different values for α (see Fig. 12), each one consistent with the previously reported one for the sample of the same origin. The liquid crystals $\bar{8}S5$, CBOOA (cyanobenzylidene-octyloxyaniline), 8CB, and CBNOA (cyanobenzylidene-nonyloxyaniline) were also measured by LeGrange and Mochel²⁴ (see Fig. 12). For CBNOA with $T_{AN}/T_{NI} = 0.99$ no α value was given, but a discontinuity in C_p and hysteresis between cooling and heating runs were reported. On the basis of their measurements, LeGrange and Mochel²⁴ arrive at the conjecture that the phase diagram can be divided in three parts. The first part consists of systems ($\bar{8}S5$, CBOOA, and one of the 8OCB samples) where some rounding was observed near T_c and where α values near zero or negative were found. A second region has sharp symmetric peaks with a large positive value for α (as for 8CB and their other 8OCB sample). The crossover between the two types of critical behavior was conjectured to occur at $T_{AN}/T_{NI} = 0.96$. It was also suggested that small differences in sample purity for 8OCB (with $T_{AN}/T_{NI} = 0.96$) could place this system in a different part of the phase diagram. A third part of the phase diagram (based on the behavior of CBNOA) would show first-order behavior for the *AN* transition with possibly a tricritical point for T_{AN}/T_{NI} between 0.99 (CBNOA) and 0.98 (8CB). Our data confirm the interpretation by LeGrange and Mochel²⁴ and previously, also, by others,²⁰ that the *AN* transition in 8CB is purely second order and that consequently the tricritical point, being the transition to the first-order part of the curve, will occur at a T_{AN}/T_{NI} value larger than that for 8CB ($T_{AN}/T_{NI} = 0.978$). The conjectured behavior for the first region is not consistent with detailed results for other systems with $T_{AN}/T_{NI} < 0.96$ (see Fig. 12). In particular, it is in disagreement with measurements for 8OCB and

mixtures of 6OCB (hexyloxybiphenyl) and 8OCB, where T_{AN}/T_{NI} could be changed by varying the pressure or the composition of the samples.^{18–21} However, the overall behavior of the α values in Fig. 12 seems to indicate an increasing α value with increasing T_{AN}/T_{NI} . This is certainly the case for the three systems of the $\bar{n}S5$ homologous series investigated by Brisbin *et al.*¹⁷ For $\bar{1}OS5$ an $\alpha \approx 0.45$ value close to the tricritical one, and indications for a first-order character, were obtained. If thus T_{AN}/T_{NI} is the only relevant parameter for all the different systems, this would mean that the tricritical value for T_{AN}/T_{NI} should be between 0.986 ($\bar{1}OS5$) and 0.978, the value for 8CB, where we do not observe a first-order discontinuity in the enthalpy curve. In order to clarify this point, measurements on systems with T_{AN}/T_{NI} values closer to 1 than the 8CB value are needed. Our measuring technique, which allows simultaneous investigation of the pretransitional effects and of the latent heat, is very well suited for it. Such measurements are in progress.

As already pointed out in Sec. I it is expected, on the basis of the analogy between the superconducting transition and the AN transition and from the renormalization-group work by Lubensky and Chen,¹¹ that the asymptotic second-order critical behavior should conform with that of the $d=3$ XY model with $\alpha = -0.02$. However, at the tricritical point between the second-order and first-order parts of the AN phase transition line, a value of $\alpha = 0.5$ would be expected. Our value of α for 8CB is not consistent with either one of these two theoretical values. As we have already pointed out before, there is in our data (see, e.g., Figs. 10 and 11) no evidence for a crossover to another α value different from our best value of 0.31. Most α values for the other systems in Fig. 12 also differ quite substantially from the XY value. Only for $\bar{8}S5$ and 8OCB agreement has been reported by some authors. For one system ($\bar{1}OS5$) an α value close to the tricritical one has been reported so far. Furthermore, the anisotropic behavior for the parallel and perpendicular correlation lengths, as observed by x-ray measurements, and the fact that anisotropic scaling holds quite well, is also in conflict with asymptotic isotropic XY or tricritical behavior. On the other hand, the very large anisotropy in the correlation length exponents expected in Eq. (1.1) does not seem to be observed experimentally.²⁷

As a final comment on the AN transition we want to consider the results obtained for the amplitude ratio A'/A . Mueller *et al.*⁵⁷ obtained for the λ tran-

sition in ${}^4\text{He}$ $A'/A = 0.90 \pm 0.02$, which is in good agreement with the less certain theoretical results (between 0.9 and 1.0) for the XY model.²⁹ Thus it follows that the specific-heat peak is rather symmetric for systems belonging to this universality class. The C_p anomaly for the AN transition is observed to be quite symmetric around T_{AN} , and deviations with the XY model are much less obvious here than for the critical exponents. Deviations from the XY value for A'/A in both directions have been reported. The results for 8CB are given in Table IV. For 8OCB, experimental values between 1.0 and 0.7 have been reported.^{19,24} For 40.8, asymmetry in opposite sense with $A'/A = 1.17$ has been obtained.²⁷ It is, however, clear that differences with the XY model are much less spectacular than in the case of the critical exponent α . For the tricritical case, a rather large asymmetry with $A'/A = 3.56$ is expected.⁵⁸ It is clear that this value is not consistent with the above experimental A'/A values for the AN transition.

C. Fits for the NI transition

We now want to compare the results of power-law fits to the pretransitional anomalies in the temperature dependence of the heat capacity near the NI transition, with the theoretical predictions and hypotheses. A power-law analysis is complicated here because of the slightly first-order character of the transition. Before the critical temperatures T_c and T'_c in the power laws Eqs. (4.1a) and (4.1b) can be reached, the first-order transition will take place at T_{NI} . The critical temperature T_c for $T > T_{NI}$ data is usually identified with T^* , the lowest possible temperature for a stable isotropic phase. T'_c is identified with T^{**} , the upper limit of stability for the nematic phase. Because direct experimental observation of T_c and T'_c is not possible, they have to be treated as adjustable parameters in the fits. Furthermore, no data points very close to T_c or T'_c will be available. This will make an accurate determination of α uncertain. In case the direct enthalpy results are analyzed, two additional free parameters H_c and H'_c , which also cannot be reached experimentally, appear as free parameters in the fits. In order to avoid an excessive number of adjustable parameters, we have chosen to analyze the heat capacity data derived by means of Eq. (2.1) from the direct $H(T)$ results. The heat capacity data of runs II, V, and VII of Table I, which agree within experimental uncertainty (see also Fig. 8), were

analyzed simultaneously. For $T < T_{\text{NI}}$, data in the temperature range between 37.3 and 40.76°C were used in the fits. For $T > T_{\text{NI}}$, the temperature range between 40.80 and 44.5°C was covered in the fits. Table V gives a survey of parameter values obtained from nonlinear least-squares fits with Eqs. (4.1a) and (4.1b). Fits 1 and 4, with α and α' free parameters, give for both these exponents values which are lower than the tricritical value $\alpha = \alpha' = 0.5$. Fits 2 and 3, and 5 and 6 where a tricritical or a $d = 3$ Ising value have been imposed for α , show that the χ_v^2 minimum is rather broad, and that α can be changed appreciably without a substantial increase in χ_v^2 , if the other parameters in the fit equation are free to adjust. A similarly large uncertainty in the α values for 8OCB was reported by Kasting *et al.*¹⁹ In this material the value of α was < 0.5 but α' was quite close to 0.5. For MBBA (*p*-methoxy-benzylidene-*p'*-*n*-butylaniline) and BMOAB (*p*-*n*-butyl-*p'*-methoxy-azoxybenzene), Anisimov *et al.*⁴⁰ reported values smaller than 0.5 for α and α' (respectively, 0.18 and 0.32 for MBBA and 0.16 and 0.38 for BMOAB). Anisimov *et al.*⁴⁰ reported very good fits to the experimental data with a crossover function between the tricritical behavior, with $\alpha = \alpha' = 0.5$, and the second-order Ising-like critical behavior, with $\alpha = \alpha' = 0.11$, of the following type:

$$\frac{C_p}{R} = \frac{1}{A_1 \epsilon^{0.5} + A_2 \epsilon^{0.11}} + B + E\epsilon \quad (4.10)$$

for $T > T_{\text{NI}}$, and an identical one with primed symbols for $T < T_{\text{NI}}$. We have also fitted our C_p/R data with these expressions. In Table VI the parameter values are given for fits to the same set of experimental data as for the fits of Table IV. Here, also, very good fits with lower χ_v^2 values are obtained. This result, together with α and α' values from Table V, show that the observed pretransitional effects in the isotropic and in the nematic phases

near T_{NI} are consistent with quasitricritical behavior. The uncertainty in the experimental α and α' values is, however, quite large.

V. SUMMARY AND CONCLUSIONS

In this paper we have presented new experimental data for the temperature dependence of the enthalpy and the heat capacity of the liquid-crystal octylcyanobiphenyl (8CB). The measurements have been carried out in the temperature range between 10 and 50°C. In this temperature range it was possible to obtain detailed results for the phase transition (KA) from the crystalline solid to the smectic-*A* phase, for the smectic-*A* to nematic (*AN*) transition, as well as for the transition (NI) from the nematic to the isotropic liquid phase. The measuring procedure described in Sec. II allowed us also to obtain accurate results for the latent heats associated with first-order transitions.

For the *KA* transition a latent heat of 25.7 ± 1.0 kJ/mol was obtained. For the NI transition a small latent heat of 612 ± 5 J/mol was measured. The *AN* transition was, within our experimental resolution, a purely continuous second-order transition. As an upper limit for the latent heat we arrive at a value of 0.4 J/mol or 1.4×10^{-3} J/g. A comparison (in Sec. III) between differential scanning calorimetric (DSC) results and our detailed enthalpy results near the three phase transitions, particularly near the *AN* transition, clearly demonstrates that the DSC results can only be considered as very qualitative.

A detailed analysis of the specific-heat anomaly near the *AN* transition was presented in Sec. IV. From a power-law analysis we obtained for the critical exponent $\alpha = \alpha' = 0.31 \pm 0.03$. The exponent value is quite insensitive to range shrinking and there is no indication of crossover to another critical behavior with a different exponent value. The

TABLE V. Parameter values from the fits with Eqs. (4.1a) and (4.1b) to the C_p/R data near the nematic-isotropic (NI) phase transition.

Fit	Phase	α, α'	A, A'	B, B'	E, E'	T_c, T'_c	χ_v^2
1	I	0.42	0.22	70.6	-1.5×10^2	40.72	1.264
2	I	(0.50) ^a	0.75	51.2	6.7×10^2	40.14	1.688
3	I	(0.11)	5.04	-11.6	8.5×10^2	40.43	1.616
4	N	0.34	1.78	56.5	1.8×10^2	40.86	0.980
5	N	(0.50)	0.67	70.7	-0.8×10^2	40.89	1.016
6	N	(0.11)	7.42	-36.0	7.4×10^2	40.82	1.025

^aParameter values between parentheses indicate that the parameter was held constant at the quoted value.

TABLE VI. Parameter values from the fits with Eq. (4.10) to the C_p/R data near the nematic-isotropic (NI) phase transition.

Parameters	$T > T_{NI}$	$T < T_{NI}$
T_c, T'_c	40.73	40.82
A_1, A'_1	3.4	0.23
A_2, A'_2	0.035	0.022
B, B'	71.7	51.1
E, E'	-1.9×10^2	4.5×10^2
χ^2_v	1.127	0.931

obtained experimental value for α is not in agreement with the nearly logarithmic singularity obtained for systems belonging to the same universality class as the XY model.^{4,57} This discrepancy

demonstrates that the critical behavior near the AN transition is more complicated than anticipated on the analogy between this transition and the superconducting-to-normal transition in a superconductor.³ Our α value can, however, be related consistently [see Eq. 4.9] with $\nu_{||}$ and ν_{\perp} values for the anisotropic correlation lengths²⁶ in 8CB via the anisotropic hyperscaling relation of Lubensky and Chen.¹¹

The analysis of the NI transition is discussed in Sec. IV C. A rather broad spectrum of α values were allowed by the data, provided that the other parameters (in particular T_c) in the fitting equation were also free to adjust. The obtained results are in qualitative agreement with the suggestions by Keyes³² and Anisimov *et al.*³⁹ of the quasitricritical character of this transition.

- ¹K. K. Kobayashi, Phys. Lett. A **31**, 125 (1970); J. Phys. Soc. Jpn. **29**, 101 (1970).
²W. L. McMillan, Phys. Rev. A **4**, 1238 (1971).
³P. G. de Gennes, Solid State Commun. **10**, 753 (1972).
⁴J. C. Le Guillou and J. Zinn-Justin, Phys. Rev. B **21**, 3976 (1980).
⁵A. Caillé, C. R. Acad. Sci. B **274**, 891 (1972).
⁶B. I. Halperin and T. C. Lubensky, Solid State Commun. **14**, 997 (1974).
⁷B. I. Halperin, T. C. Lubensky, and S.-K. Ma, Phys. Rev. Lett. **32**, 292 (1974).
⁸C. Dasgupta and B. I. Halperin, Phys. Rev. Lett. **47**, 1556 (1981).
⁹W. Helfrich, J. Phys. (Paris) **39**, 1199 (1978).
¹⁰D. R. Nelson and J. Toner, Phys. Rev. B **24**, 363 (1981).
¹¹T. C. Lubensky and J. H. Chen, Phys. Rev. B **17**, 366 (1978).
¹²J. H. Chen, T. C. Lubensky, and D. R. Nelson, Phys. Rev. B **17**, 4274 (1978).
¹³S. G. Dunn and T. C. Lubensky, J. Phys. (Paris) **42**, 1201 (1981).
¹⁴T. C. Lubensky, S. C. Dunn, and J. Isaacson, Phys. Rev. Lett. **47**, 1609 (1981).
¹⁵D. L. Johnson, C. F. Hayes, R. J. DeHoff, and C. A. Schantz, Phys. Rev. B **18**, 4902 (1978).
¹⁶C. A. Schantz and D. L. Johnson, Phys. Rev. A **17**, 1504 (1978).
¹⁷D. Brisbin, R. DeHoff, T. E. Lockhart, and D. L. Johnson, Phys. Rev. Lett. **43**, 1171 (1979).
¹⁸C. W. Garland, G. B. Kasting, and K. J. Lushington, Phys. Rev. Lett. **43**, 1420 (1979).
¹⁹G. B. Kasting, K. J. Lushington, and C. W. Garland, Phys. Rev. B **22**, 321 (1980).
²⁰G. B. Kasting, C. W. Garland, and K. J. Lushington, J. Phys. (Paris) **41**, 879 (1980).
²¹K. J. Lushington, G. B. Kasting, and C. W. Garland, Phys. Rev. B **22**, 2569 (1980).
²²K. J. Lushington, G. B. Kasting, and C. W. Garland, J. Phys. (Paris) Lett. **41**, L419 (1980).
²³E. Bloemen and C. W. Garland, J. Phys. (Paris) **42**, 1299 (1981).
²⁴J. D. LeGrange and J. M. Mochel, Phys. Rev. Lett. **45**, 35 (1980); Phys. Rev. A **23**, 3215 (1981).
²⁵I. Hatta and T. Nakayama, Mol. Cryst. Liq. Cryst. **66**, 97 (1981).
²⁶D. Davidov, C. R. Safinya, M. Kaplan, S. S. Dana, R. Schaetzing, R. J. Birgeneau, and D. Litster, Phys. Rev. B **19**, 1657 (1979); J. D. Litster, J. Als-Nielsen, R. J. Birgeneau, S. S. Dana, D. Davidov, F. Garcia-Golding, M. Kaplan, C. R. Safinya, and R. Schaetzing, J. Phys. (Paris) Colloq. **40**, C3-339 (1979).
²⁷R. J. Birgeneau, C. W. Garland, G. B. Kasting, and B. M. Ocko, Phys. Rev. A **24**, 2624 (1981), and references therein.
²⁸H. Birecki, R. Schaetzing, F. Rondelez, and J. D. Litster, Phys. Rev. Lett. **36**, 1376 (1976); H. von Känel and J. D. Litster, Phys. Rev. A **23**, 3251 (1981).
²⁹D. Stauffer, M. Ferer, and M. Wortis, Phys. Rev. Lett. **29**, 345 (1972); P. C. Hohenberg, A. Aharony, B. I. Halperin, and E. D. Siggia, Phys. Rev. B **13**, 2986 (1976).
³⁰P. G. de Gennes, Phys. Lett. A **30**, 454 (1969); Mol. Cryst. Liq. Cryst. **12**, 193 (1971).
³¹P. G. de Gennes, *The Physics of Liquid Crystals* (Clarendon, Oxford, 1974).
³²P. H. Keyes, Phys. Lett. A **67**, 132 (1978).
³³C. Fan and M. J. Stephen, Phys. Rev. Lett. **25**, 500 (1970); R. G. Priest, Phys. Lett. A **47**, 475 (1974).
³⁴G. R. Van Hecke and J. Stecki, Phys. Rev. A **25**, 1123 (1982).

- ³⁵P. H. Keyes and J. R. Shane, *Phys. Rev. Lett.* **42**, 722 (1979).
- ³⁶I. Haller, *Prog. Solid State Chem.* **10**, 103 (1975).
- ³⁷G. Koren, *Phys. Rev. A* **13**, 1177 (1976).
- ³⁸B. I. Ostrovskii, S. A. Taraskin, B. A. Strukov, and A. S. Sonin, *Zh. Eksp. Teor. Fiz.* **71**, 692 (1976) [*Sov. Phys.—JETP* **44**, 363 (1977)].
- ³⁹M. A. Anisimov, S. R. Garber, V. S. Esipov, V. M. Mammitskii, G. I. Ovodov, L. A. Smolenko, and E. L. Sorokin, *Zh. Eksp. Teor. Fiz.* **72**, 1983 (1977) [*Sov. Phys.—JETP* **45**, 1042 (1977)].
- ⁴⁰M. A. Anisimov, V. M. Mammitskii, and E. L. Sorokin, *J. Eng. Phys. (USSR)* **39**, 1385 (1981).
- ⁴¹J. Thoen, E. Bloemen, and W. Van Dael, *J. Chem. Phys.* **68**, 735 (1978).
- ⁴²E. Bloemen, J. Thoen, and W. Van Dael, *J. Chem. Phys.* **75**, 4628 (1980).
- ⁴³E. Bloemen, J. Thoen, and W. Van Dael, *J. Chem. Phys.* **75**, 1488 (1981).
- ⁴⁴Apparently an indirect indication of the existence of not too small first-order latent heats, as, e.g., for the NI transition, can be obtained from anomalous phase shifts in the T_{ac} signal. For details see Ref. 19.
- ⁴⁵J. Thoen, E. Bloemen, H. Marynissen, and W. Van Dael, *Proceedings of the 8th Symposium of Thermophysical Properties, Natl. Bur. Stand., Maryland, 1981*, (American Society of Mechanical Engineers, New York, 1982).
- ⁴⁶N. S. Osborne, H. F. Stimson, and D. C. Ginnings, *Natl. Bur. Stand. J. Res.* **23**, 238 (1939).
- ⁴⁷L. Liebert and W. B. Daniels, *J. Phys. (Paris) Lett.* **38**, L333 (1977).
- ⁴⁸H. J. Coles and C. Strazielle, *Mol. Cryst. Liq. Cryst.* **55**, 237 (1979).
- ⁴⁹G. W. Smith, *Mol. Cryst. Liq. Cryst.* **41**, 89 (1977).
- ⁵⁰A. J. Leadbetter, J. L. Durrant, and M. Rugman, *Mol. Cryst. Liq. Cryst. (Lett.)* **34**, 231 (1977).
- ⁵¹D. A. Dunmur and W. H. Miller, *J. Phys. (Paris) Colloq.* **40**, C3-141 (1979).
- ⁵²We thank Professor C. W. Garland for making the numerical values of their 8CB results available to us.
- ⁵³It may be of interest to note that the 8CB sample for the ac measurements had also been obtained from BDH Chemicals, and had the same batch number as ours.
- ⁵⁴F. J. Wegner, *Phys. Rev. B* **5**, 4529 (1972).
- ⁵⁵We used the CERN computer MINUIT, CERN Computer Center program library No. 506.
- ⁵⁶D. Djurek, J. Baturić-Rubčić, and K. Franulović, *Phys. Rev. Lett.* **33**, 1126 (1974).
- ⁵⁷K. H. Mueller, F. Pobell, and G. Ahlers, *Phys. Rev. Lett.* **34**, 513 (1975); *Phys. Rev. B* **14**, 2096 (1976); G. Ahlers, *Rev. Mod. Phys. Lett.* **52**, 489 (1980).
- ⁵⁸E. E. Gorodetskii and V. M. Zaprudskii, *Zh. Eksp. Teor. Fiz.* **72**, 2299 (1977) [*Sov. Phys.—JETP* **45**, 1209 (1977)].